Electronic Supplementary Material (ESI) for RSC Advances.

Supporting Information

Characterization of sulfur/carbon copolymer cathodes for Li-S batteries: a combined experimental and ab initio Raman spectroscopy study

Rana Kiani, Matthias Steimecke, Marah Alqaisi, Michael Bron, Daniel Sebastiani, and Pouya Partovi-Azar*

Institute of Chemistry, Martin Luther University Halle-Wittenberg, Von-Danckelmann-Platz 4, 06120 Halle (Saale), Germany

E-mail: pouya.partovi-azar@chemie.uni-halle.de

Raman spectroscopy simulations

Assignment of Raman peaks

Wannier polarizability method provides a simple and straightforward way for the assignment of Raman peaks. The procedure is shown in Fig. 1 for S_4 chain. The lower panel schematically shows three Wannier functions localized on three S–S bond. Local Raman-active vibrations corresponding to each Wannier function can be obtained by including their spread into the summation $\bar{A} = \frac{1}{3}\mathrm{Tr}[A] = \frac{\beta}{3}\sum_{n=1}^{N_{\mathrm{WF}}} S_n^3$ to obtain the local mean polarizability, $\bar{A}$. S_n are the Wannier spreads and β is found to be $\simeq$0.9.[1–3] These vibrations mainly include

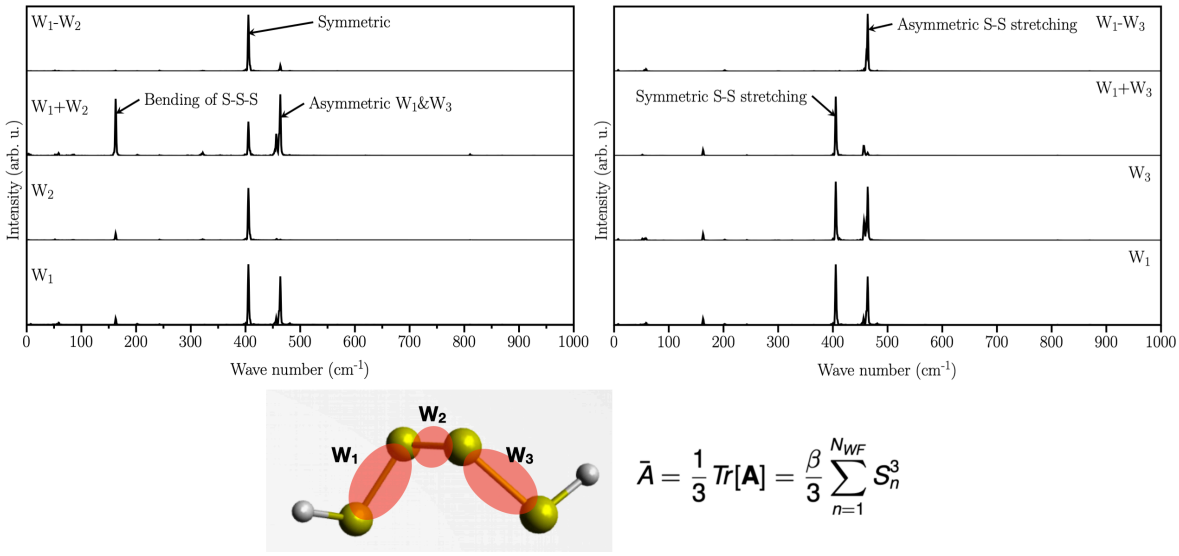

Figure 1: Assignment of Raman-active peaks using Wannier polarizability method.

stretching vibrations. Therefore, in Fig. 1, they are assigned to symmetric ans antisymmetric vibrations. Due to symmetry restrictions, W_2 only shows a single stretching at $\sim$400 cm^{-1}. However, W_1 and W_3 show two vibrations in 400-500 cm^{-1} range corresponding to symmetric and antisymmetric stretching. In order to distinguish between them, one can include in the above summation combinations S_1+S_3 and S_1+(-S_3). In the former case, the partial spectrum only shows an activity around 400 cm^{-1}, while in the latter case, the activity is only seen at $\sim$460 cm^{-1}. Therefore, we assign the peak at around 400 cm^{-1} to symmetric S-S stretching and the one at $\sim$460 cm^{-1} to an antisymmetric one. The Raman activities at lower frequencies can be assigned to longer-range vibrations by including more Wannier functions in the polarizability summation.

Figure 2 shows the partial Raman spectrum corresponding to the propyl (red) and propenyl (black) groups in 1,3-diisopropylbenzene and 1,3-diisopropenylbenzene molecules, respectively. Presence of the peak $\sim$450 cm^{-1} in the partial Raman spectrum of propyl groups shows this activity arises from a CH_3 vibration. Note that this peak is much less intensive in the partial spectrum of propenyl group (black) [also see Fig. 1(a) in the main text].

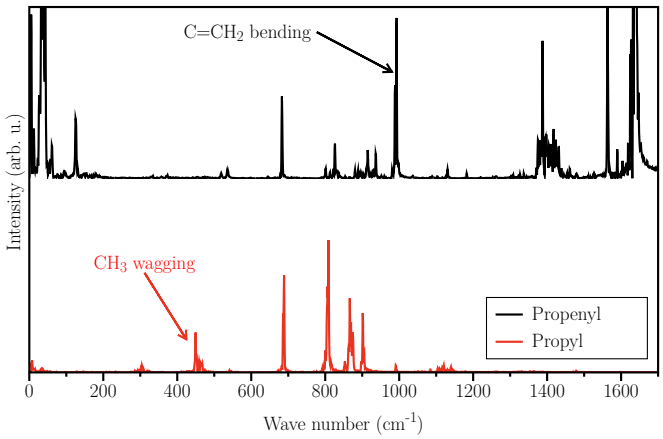

Figure 2: Partial Raman spectra of propyl and propenyl groups in 1,3-diisopropylbenzene and 1,3-diisopropenylbenzene molecules.

Elemental analysis and ^{1}H NMR spectroscopy

Elemental analyses were performed by the Central Analytical Services of the Institute of Chemistry of the MLU on an UNICUBE CHN(S) analyzer (by Elementar) using argon as carrier/shielding gas and tin-foil crucibles for sample preparation (2mg scale, with sulfanilamide as reference substance) see Table 1.

Table 1: Elemental analyses of synthesized Sufur co-polymer.

System	C wt%	H wt%	S wt%
SDID20	18.22	1.756	80.331
SDIB25	23.00	2.200	76.653
SDIB30	26.30	2.537	72.886
SDIB40	34.82	3.377	61.804
SDIB50	43.97	4.291	52.323

To confirm the formation of copolymers and C-S bonds, we measure ^{1}H NMR spectra of SDIBw samples, w = 20, 25, 30, 40, and 50 (Fig. 3). Although NMR spectroscopy provides good structural information on aromatic and aliphatic functional groups, it is not easy to fully assign all the peaks because of the complexity of the cross-linked sulfur copolymers. Figure 3 confirms the presence of aromatic hydrogens at $\delta = 7.0 - 7.5$ ppm and methyl protons at $\delta = 1.5 - 2.0$ ppm. NMR shifts at $\delta = 2.2$ ppm correspond to the methylene

protons in DIB and, consequently, the formation of C-S bonds. Moreover, two subordinate peaks at $\delta = 5.0 - 5.5$ illustrate the excess amount of DIB as a monomer in the samples. In other words, it is an evidence for C=C bonds, which remained unreacted with sulfur chains. Also, the NMR intensity of peaks at $\delta = 2.2$ and $\delta = 5.0 - 5.5$ ppm increases by increasing the total wt % of DIB in the sample. This means in samples with a higher wt % of monomer, the chance of C-S bonds formation is higher. Nevertheless, some of the C=C bonds of the monomer stay unsaturated.

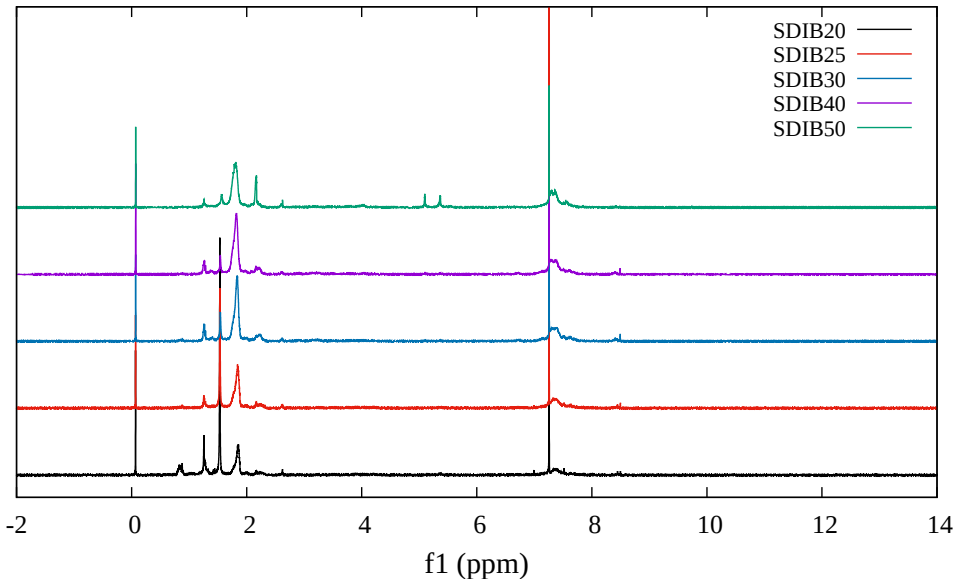

Figure 3: ^{1}H NMR spectra of SDIBw copolymers with different wt % of DIB in $CDCl_3$.

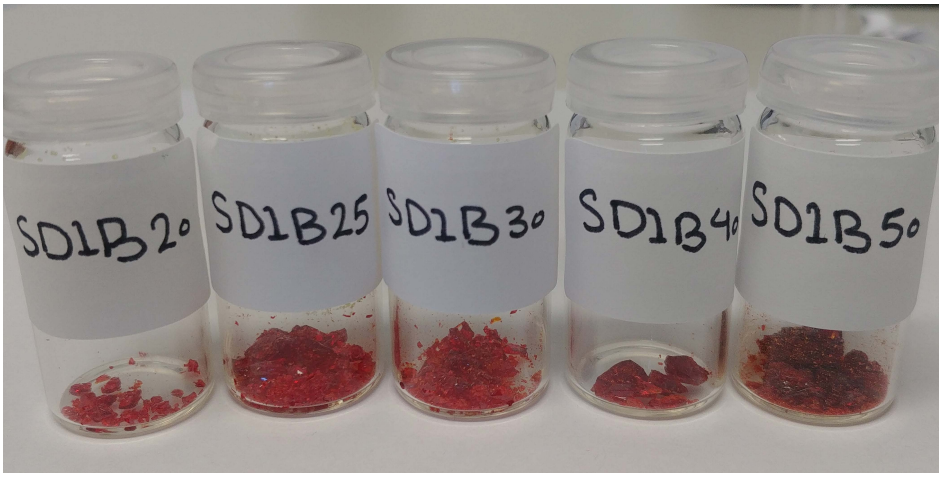

Figure 4: Pictures of synthesised SDIBw copolymers with different wt % of DIB, showing slight change in their color by increasing DIB amount.

Raman Spectroscopy measurements

Figure 5 shows the experimental Raman spectra of SDIBw with different DIB wt % of (a) SDIB20, (b) SDIB25, (c) SDIB30, (d) SDIB40, and (e) SDIB50. Different colors correspond to spectra measured at different positions of each sample. A notable difference between the spectrum shown in red and those in black and blue is seen in the case of SDIB20 in Fig. 5(a). We have performed X-ray diffraction measurements to inspect possible crystallinity in SDIB20 and SDIB40 samples (see below).

Crystallinity analysis of S/DIB copolymers

To provide more information on the molecular structure of S/DIB copolymers, including the symmetry of its vibrational modes and its crystallinity, additional polarized Raman spectroscopy measurements on SDIB20 were performed (Fig. 6). The laser beam emission was in normal, circular, and orthogonal directions. Probing the 10 μm triangular-shaped part of the sample shows the dependency of polarization which may imply that this sample or part of it could be crystalline.

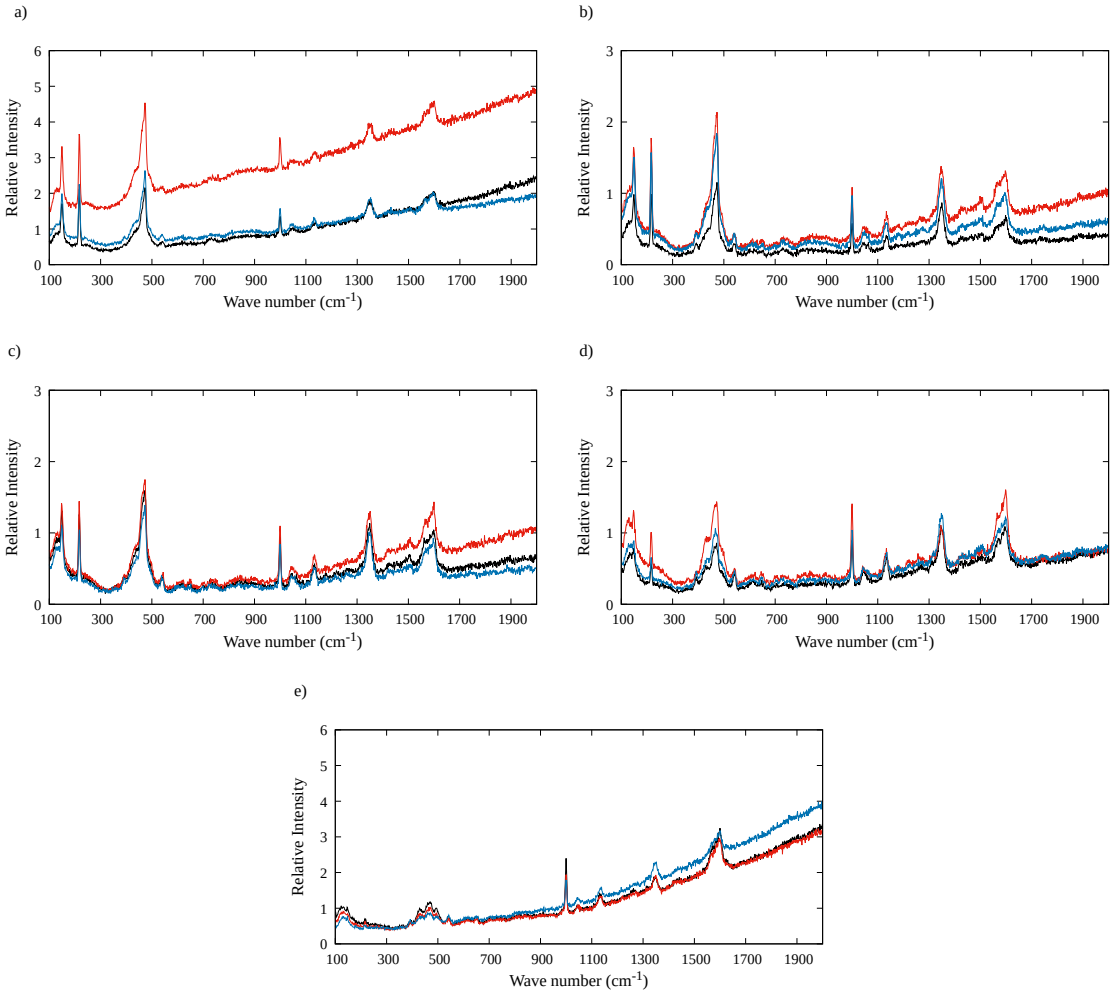

Figure 5: Measured Raman spectra of SDIBw with different wt % of DIB. (a) SDIB20, (b) SDIB25, (c) SDIB30, (d) SDIB40, and (e) SDIB50. Different colors show spectra measured at different positions of each sample.

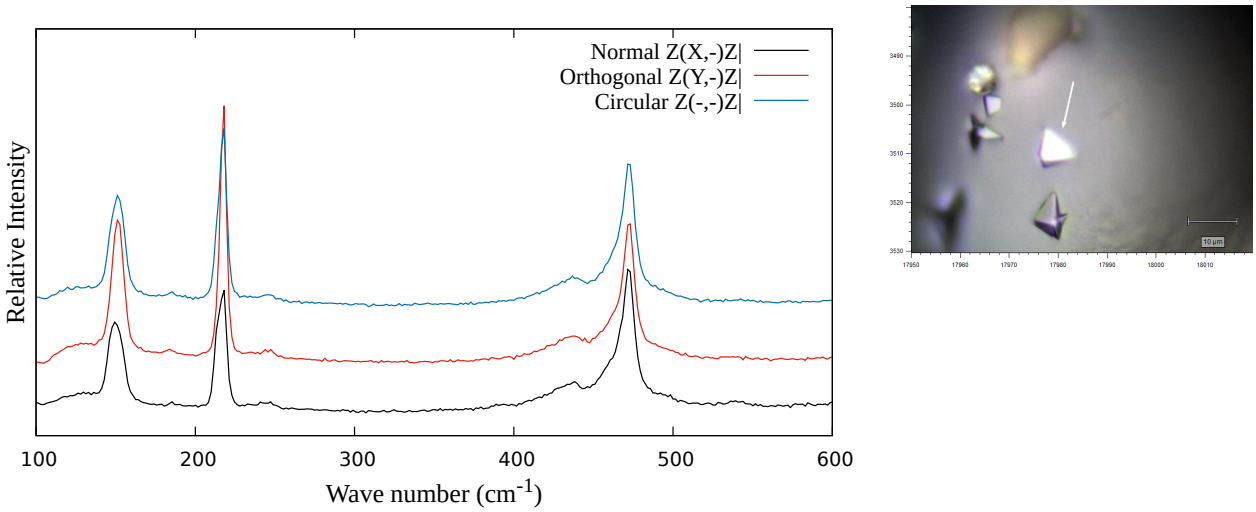

Figure 6: Polarised Raman Spectrum of SDIB20.

In addition, X-ray diffraction (XRD) measurements on SDIB20 and SDIB40 were performed to examine their crystallinity (λ= 1.5406 Å). Fig. 7 shows single crystal XRD pattern for (a) SDIB20 and (b) SIB40. Fig. 7(a) illustrates that SDIB20 might contain crystals, but the observed reflexes could sometimes be related to the background. Moreover, none of the other measurements show similar signals. Also, it could be related to excess amount of crystalline sulfur in the sample.[4] For example, single particle XRD pattern of SDIB40 [Fig. 7(b)] shows a clear amorphous structure.

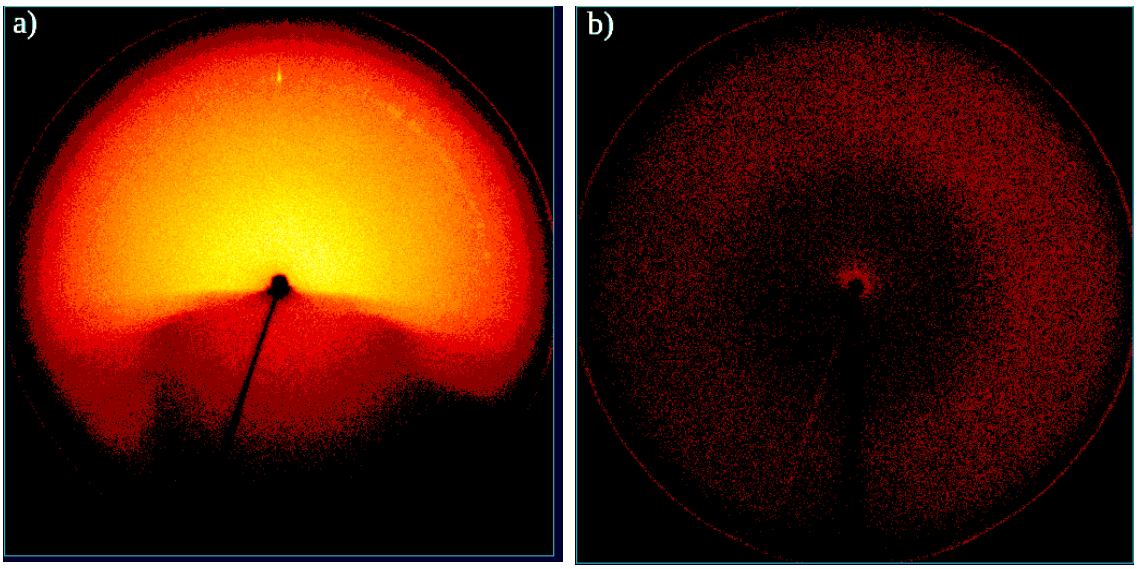

Figure 7: Single crystal XRD pattern of (a) SDIB20 and (b) SIB40.

Fig. 8 shows the same measurement but with integrated intensity and background is subtracted. Because of the absence of a periodic arrangement in amorphous materials, only higher diffraction angles are signified in the XRD graph. Therefore, it clearly presents the XRD graphs of an amorphous structure.

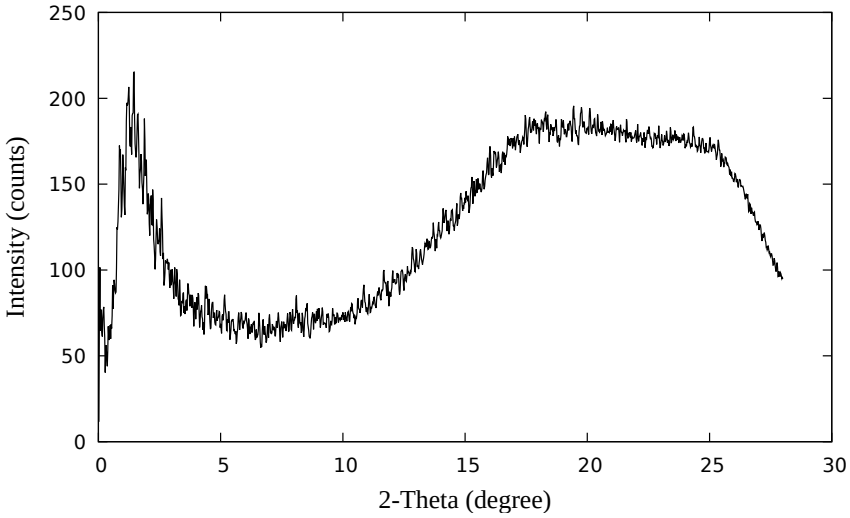

Figure 8: XRD qualitative graph for SDIB40.

References

(1) Partovi-Azar, P.; Kühne, T. D. Efficient "On-the-Fly" calculation of Raman Spectra from Ab-Initio molecular dynamics: Application to hydrophobic/hydrophilic solutes in bulk water. *Journal of Computational Chemistry* **2015**, *36*, 2188–2192.

(2) Partovi-Azar, P.; Kühne, T. D.; Kaghazchi, P. Evidence for the existence of Li 2 S 2 clusters in lithium–sulfur batteries: ab initio Raman spectroscopy simulation. *Physical Chemistry Chemical Physics* **2015**, *17*, 22009–22014.

(3) Partovi-Azar, P.; Kühne, T. D. Full Assignment of Ab-Initio Raman Spectra at Finite Temperatures Using Wannier Polarizabilities: Application to Cyclohexane Molecule in Gas Phase. *Micromachines* **2021**, *12*, 1212.

(4) Rafie, A.; Pereira, R.; Shamsabadi, A. A.; Kalra, V. In Operando FTIR Study on the Effect of Sulfur Chain Length in Sulfur Copolymer-Based Li–S Batteries. *The Journal of Physical Chemistry C* **2022**, *126*, 12327–12338.